Unconventional plasmon-phonon coupling in graphene

Jablan, Marinko; Soljačić, Marin; Buljan, Hrvoje

Source / Izvornik: **Physical review B: Condensed matter and materials physics, 2011, 83**

Journal article, Published version
Rad u časopisu, Objavljena verzija rada (izdavačev PDF)

https://doi.org/10.1103/PhysRevB.83.161409

Permanent link / Trajna poveznica: https://urn.nsk.hr/urn:nbn:hr:217:267734

PHYSICAL REVIEW B **83**, 161409(R) (2011)

Unconventional plasmon-phonon coupling in graphene

Marinko Jablan,[1,*] Marin Soljačić,[2,†] and Hrvoje Buljan[1,‡]
[1]*Department of Physics, University of Zagreb, Bijenička c. 32, 10000 Zagreb, Croatia*
[2]*Department of Physics, Massachusetts Institute of Technology, 77 Massachusetts Avenue, Cambridge Massachusetts 02139, USA*
(Received 19 March 2011; published 27 April 2011)

We predict the existence of coupled plasmon-phonon excitations in graphene by using the self-consistent linear response formalism. The unique electron-phonon interaction in graphene leads to unconventional mixing of plasmon and optical phonon polarizations. We find that longitudinal plasmons couple exclusively to transverse optical phonons, whereas graphene's transverse plasmons couple only to longitudinal optical phonons. This coupling can serve as a magnifier for exploring the electron-phonon interaction in graphene, and it offers electronical control over phonon frequencies.

DOI: 10.1103/PhysRevB.83.161409 PACS number(s): 73.20.Mf, 73.22.Lp, 63.22.Rc, 78.67.Wj

The interaction of electrons and crystal lattice vibrations (phonons) has fundamental implications for properties of materials and leads to diverse many-body phenomena, such as superconductivity and charge-density waves. The electron-phonon interaction takes an unusual form in graphene, a recently discovered two-dimensional (2D) material[1] (see, e.g., Ref. 2 for a review), and its implications are far from being explored. These include the breakdown of the Born-Oppenheimer approximation,[3] the anomaly of the optical phonon,[4] and the nonadiabatic Khon anomaly.[5] However, the interaction of collective electron excitations (plasmons) and optical phonons has not yet been presented for graphene. Plasmons in graphene are of fundamental scientific interest,[6–12] but they also hold potential for technological applications (e.g., in the context of plasmon lasers[9] and metamaterials[12]). Besides the ordinary longitudinal plasmons (transverse magnetic modes),[6–9,12] graphene also supports unusual transverse plasmons (transverse electric modes).[8] The hybridization of plasmon and phonon modes is a striking manifestation of the breakdown of the Born-Oppenheimer approximation because it occurs when phonons and electrons are on comparable energy scales. Plasmon-phonon coupling has been studied in bulk semiconductors[13,14] and systems with reduced dimensionality (see, e.g., Refs. 15–18), and in the context of graphene, plasmons were shown to couple to surface optical phonons of the substrate (e.g., SiC, which is a polar material).[11,19,20] Here we predict the coupling of plasmons with intrinsic optical phonons in graphene by using the self-consistent linear response formalism. We find that, in contrast to all other known systems in nature, longitudinal plasmons (LP) couple only to transverse optical (TO) phonons,[21] while transverse plasmons (TPs) couple only to longitudinal optical (LO) phonons. The LP-TO coupling is stronger for larger concentration of carriers, in contrast to the TP-LO coupling (which is fairly weak). The former could be measured via current experimental techniques. Thus, plasmon-phonon resonance could serve as a magnifier for exploring the electron-phonon interaction and for electronic control (by externally applied voltage) over crystal lattice vibrations in graphene.

The low-energy band structure of graphene consists of two degenerate Dirac cones at K and K' points of the Brillouin zone[22,23] [see Figs. 1(a) and 1(b)], and the electron Hamiltonian around K point can be written as

$$H_e = \hbar v_F \boldsymbol{\sigma} \cdot \mathbf{k}, \tag{1}$$

where $v_F = 10^6$ m/s, $\mathbf{k} = (k_x, k_y) = -i\nabla$ is the wave-vector operator, $\boldsymbol{\sigma} = (\sigma_x, \sigma_y)$, and $\sigma_{x,y}$ are the Pauli spin matrices. We label the eigenstates of Hamiltonian H_e by $|s,\mathbf{k}\rangle$ and the appropriate eigenvalues by $E_{s,\mathbf{k}} = s\hbar v_F|\mathbf{k}|$, where $s = 1$ for the conduction band and $s = -1$ for the valence band. A technologically interesting property of graphene is that the concentration of electrons n, and hence the Fermi level $E_F = \hbar v_F \sqrt{\pi n}$, can be changed via gate voltage.[1]

The long-wavelength in-plane optical phonon branch in graphene consists of two modes (LO and TO), which are effectively dispersionless and degenerate at energy $\hbar\omega_0 = 0.196$ eV.[24,25] Let $\mathbf{u}(\mathbf{R}) = [\mathbf{u}_A(\mathbf{R}) - \mathbf{u}_B(\mathbf{R})]/\sqrt{2}$ denote the relative displacements of the sublattice atoms A and B of a unit cell specified by a coordinate $\mathbf{R}$ [see Fig. 1(c)]. Then, in the long-wavelength limit $\mathbf{R}$ can be replaced with a continuous coordinate $\mathbf{r}$ and we have

$$\mathbf{u}(\mathbf{r}) = \sum_{\mu\mathbf{q}} \frac{1}{\sqrt{NM}} Q_{\mu\mathbf{q}} \mathbf{e}_{\mu\mathbf{q}} e^{i\mathbf{qr}}, \tag{2}$$

where N is the number of unit cells, M is the carbon atom mass, $\mathbf{q} = q(\cos\phi_{\mathbf{q}}, \sin\phi_{\mathbf{q}})$ is the phonon wave vector, $\mu = L, T$ stands for the polarization, and the polarization unit vectors are $\mathbf{e}_{L\mathbf{q}} = i(\cos\phi_{\mathbf{q}}, \sin\phi_{\mathbf{q}})$ and $\mathbf{e}_{T\mathbf{q}} = i(-\sin\phi_{\mathbf{q}}, \cos\phi_{\mathbf{q}})$. The displacement vector $\mathbf{u}(\mathbf{r})$ is parallel (perpendicular) to the phonon propagation wave vector $\mathbf{q}$ for LO (TO, respectively) phonons [see Fig. 1(c)]. The phonon Hamiltonian is given by

$$H_{ph} = \frac{1}{2} \sum_{\mu\mathbf{q}} \left(P^\dagger_{\mu\mathbf{q}} P_{\mu\mathbf{q}} + \omega_0^2 Q^\dagger_{\mu\mathbf{q}} Q_{\mu\mathbf{q}} \right), \tag{3}$$

where $Q_{\mu\mathbf{q}}$ and $P_{\mu\mathbf{q}}$ denote phonon coordinate and momentum. The electron-phonon interaction takes a peculiar form in graphene[25]

$$H_{e-ph} = -\sqrt{2}\frac{\beta\hbar v_F}{b^2} \boldsymbol{\sigma} \times \mathbf{u}(\mathbf{r}), \tag{4}$$

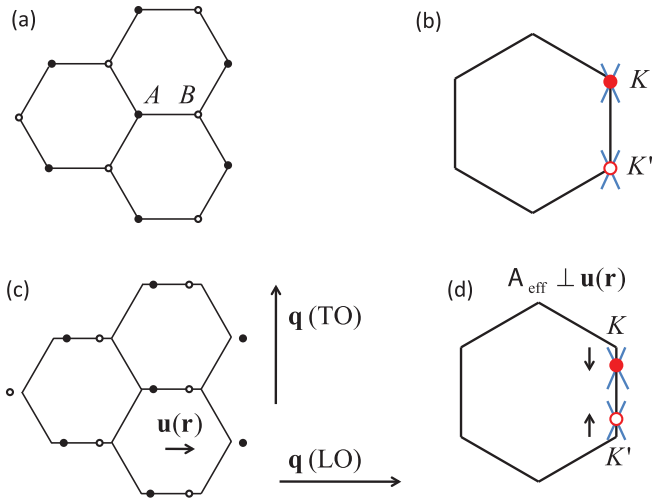

FIG. 1. (Color online) (a) Schematic illustration of the lattice structure with two sublattices (A and B). (b) The two degenerate Dirac cones are centered at K and K' points at the edge of the Brillouin zone. (c) A displacement of lattice atoms $\mathbf{u}(\mathbf{r})$ is parallel (perpendicular) to the propagation wave vector $\mathbf{q}$ of a LO (TO) phonon. (d) The displacement $\mathbf{u}(\mathbf{r})$ creates an effective vector potential $\mathbf{A}_{\text{eff}}$ *perpendicular* to $\mathbf{u}(\mathbf{r})$ (the sign of $\mathbf{A}_{\text{eff}}$ for the K' point is opposite to that for the K point).

where $\boldsymbol{\sigma}\times\mathbf{u}=\sigma_x u_y-\sigma_y u_x$, $b=0.142$ nm is the nearest carbon atoms distance, and $\beta=2$. We find it convenient to write Eq. (4) as

$$H_{e-ph}=L^2F\sum_{\mu\mathbf{q}}\mathbf{j}^\dagger_{\mathbf{q}}\times\mathbf{e}_{\mu\mathbf{q}}Q_{\mu\mathbf{q}}, \tag{5}$$

where $\mathbf{j}_{\mathbf{q}}=-ev_FL^{-2}\boldsymbol{\sigma}e^{-i\mathbf{qr}}$ is the single-particle current-density operator, L^2 is the area of the system, $-e$ is charge of the electron, and $F=\frac{\sqrt{2}\beta\hbar}{eb^2\sqrt{NM}}$.

The electromagnetic field in the plane of graphene is completely described by the vector potential $\mathbf{A}=\sum_{\mu\mathbf{q}}\mathbf{e}_{\mu\mathbf{q}}A_{\mu\mathbf{q}}e^{i\mathbf{qr}}$ (scalar potential is gauged to zero, time dependence is implicitly assumed, and $\mu=L,T$ denote polarizations). The interaction with Dirac electrons is obtained by substitution $\hbar\mathbf{k}\to\hbar\mathbf{k}+e\mathbf{A}$ in Eq. (1), which leads to

$$H_{e-em}=ev_F\boldsymbol{\sigma}\cdot\mathbf{A}=-L^2\sum_{\mu\mathbf{q}}\mathbf{j}^\dagger_{\mathbf{q}}\cdot\mathbf{e}_{\mu\mathbf{q}}A_{\mu\mathbf{q}}. \tag{6}$$

By comparing Eqs. (4) and (6) it follows that electron-phonon interaction can be regarded as a presence of an effective vector potential,

$$\mathbf{A}_{\text{eff}}=F\sum_{\mathbf{q}}\left(\mathbf{e}_{T\mathbf{q}}Q_{L\mathbf{q}}-\mathbf{e}_{L\mathbf{q}}Q_{T\mathbf{q}}\right)e^{i\mathbf{qr}}, \tag{7}$$

that is, $H_{e-ph}=ev_F\boldsymbol{\sigma}\cdot\mathbf{A}_{\text{eff}}$. It is evident that $\mathbf{A}_{\text{eff}}\cdot\mathbf{u}(\mathbf{r})=0$ that is the effective vector potential $\mathbf{A}_{\text{eff}}$ is perpendicular to $\mathbf{u}(\mathbf{r})$ as illustrated in Figs. 1(c) and 1(d) (see also Ref. 2), which is responsible for the mixing of polarizations in plasmon-phonon coupling. This result is strictly valid only in the long-wavelength limit.

As a first pass, let us ignore the phonons and focus on the Hamiltonian $H=H_e+H_{e-em}$. Without an external perturbation, the electrons in graphene fill the Fermi sea according to the Fermi distribution function $f_{s\mathbf{k}}$. A field $A_{\mu\mathbf{q}}(\omega)$ oscillating at frequency ω will induce an average current density (up to a linear order in the vector potential)

$$\langle J_\mu(\mathbf{q},\omega)\rangle=-\chi_\mu(\mathbf{q},\omega)A_{\mu\mathbf{q}}(\omega), \tag{8}$$

where the current-current response function (including two-spin and two-valley degeneracy) is given by[26]

$$\chi_\mu(\mathbf{q},\omega)=4L^2\sum_{s_1s_2\mathbf{k}}\frac{f_{s_1\mathbf{k}}-f_{s_2\mathbf{k}+\mathbf{q}}}{\hbar\omega+\hbar\omega_{s_1\mathbf{k}}-\hbar\omega_{s_2\mathbf{k}+\mathbf{q}}+i\eta}\times|\langle s_1\mathbf{k}|\mathbf{j}_{\mathbf{q}}\cdot\mathbf{e}^*_{\mu\mathbf{q}}|s_2\mathbf{k}+\mathbf{q}\rangle|^2. \tag{9}$$

For the response function $\chi_\mu(\mathbf{q},\omega)$ we utilize the analytical expression from Ref. 27. The subtlety involved with the divergence in Eq. (9) is solved by subtracting from $\chi_L(\mathbf{q},\omega)$ $[\chi_T(\mathbf{q},\omega)]$ the value $\chi_L(\mathbf{q},\omega=0)$ $[\chi_T(\mathbf{q}\to0,\omega=0)]$ to take into account that there is no current response to the longitudinal [transverse] time [time and space] independent vector potential (see Refs. 27 and 28 for details). We would like to note that when working with the current-current response function, rather than with the density-density response function, the nature of the plasmon-phonon interaction (especially the mixing of polarizations as shown below) is far more transparent.

Next, it is straightforward to show from the Maxwell equations that an electric current oscillating in a 2D plane will induce a vector potential

$$\left\langle A_{L\mathbf{q}}(\omega)\right\rangle=\langle J_L(\mathbf{q},\omega)\rangle\frac{\sqrt{q^2-\omega^2/c^2}}{-2\omega^2\epsilon_0}, \tag{10}$$

and

$$\left\langle A_{T\mathbf{q}}(\omega)\right\rangle=\langle J_T(\mathbf{q},\omega)\rangle\frac{\mu_0}{2\sqrt{q^2-\omega^2/c^2}}, \tag{11}$$

where we have assumed that graphene is suspended in air and that there are no other sources present in space. This induced vector potential in turn acts on electrons in graphene through the interaction Hamiltonian H_{e-em}, which can result in plasmons, self-sustained collective oscillations of electrons. From Eqs. (8) and (10) we get the dispersion relation for longitudinal plasmons[6,7,12]

$$1-\frac{\sqrt{q^2-\omega^2/c^2}}{2\omega^2\epsilon_0}\chi_L(\mathbf{q},\omega)=0. \tag{12}$$

From Eqs. (8) and (11) we get the dispersion relation for TPs:[8]

$$1+\frac{\mu_0}{2\sqrt{q^2-\omega^2/c^2}}\chi_T(\mathbf{q},\omega)=0. \tag{13}$$

Longitudinal plasmons are also referred to as transverse magnetic modes since they are accompanied by a longitudinal electric (E) and a transverse magnetic field (B) in the plane of graphene. Likewise, TPs or transverse electric modes are accompanied by a transverse electric and a longitudinal magnetic field.[8] Dispersion relation of LP (TP) modes is shown by the blue dashed line in Fig. 2. (Figure 3, respectively.) Finally we note that we are primarily interested in nonradiative modes ($q>\omega/c$) in which case fields are localized near the graphene plane ($z=0$) and decay exponentially: $E(z),B(z)\propto e^{-|z|\sqrt{q^2-\omega^2/c^2}}$.

In order to find the plasmon-phonon coupled excitations we consider the complete Hamiltonian $H=H_e+H_{e-em}+$

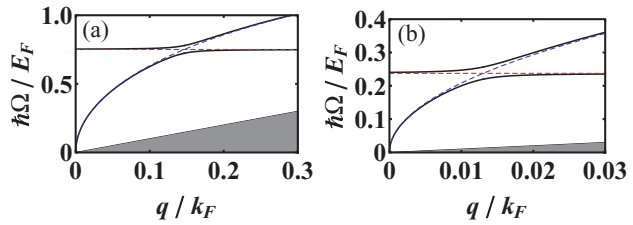

FIG. 2. (Color online) Dispersion lines of hybrid LP-TO plasmon-phonon modes (solid lines) and of the uncoupled modes (dashed lines) for two values of doping: (a) $n = 5 \times 10^{12}$ cm^{-2} and (b) $n = 5 \times 10^{13}$ cm^{-2}. The hybridization is stronger for larger doping values. Gray areas denote the region of single-particle damping.

$H_{e-ph} + H_{ph}$. We assume that the hybrid plasmon phonon mode oscillates at some frequency ω with wave vector q. From the equation of motion for the phonon amplitudes $Q_{\mu\mathbf{q}}$ one finds[26]

$$\left(\omega^2 - \omega_0^2\right)\langle Q_{T\mathbf{q}}\rangle = L^2 F \langle J_L(\mathbf{q},\omega)\rangle, \tag{14}$$

and

$$\left(\omega^2 - \omega_0^2\right)\langle Q_{L\mathbf{q}}\rangle = -L^2 F \langle J_T(\mathbf{q},\omega)\rangle. \tag{15}$$

The electron phonon interaction (5) is included as the effective vector potential (7) in Eq. (6), which from Eq. (8) immediately yields

$$\langle J_L(\mathbf{q},\omega)\rangle = \chi_L(\mathbf{q},\omega)\big(-\langle A_{L\mathbf{q}}(\omega)\rangle + F\langle Q_{T\mathbf{q}}\rangle\big), \tag{16}$$

and

$$\langle J_T(\mathbf{q},\omega)\rangle = \chi_T(\mathbf{q},\omega)\big(-\langle A_{T\mathbf{q}}(\omega)\rangle - F\langle Q_{L\mathbf{q}}\rangle\big). \tag{17}$$

From Eqs. (14)–(17) it is clear that transverse (longitudinal) phonons couple only to longitudinal (transverse) plasmons. Apparently, this follows from the fact that LO (TO, respectively) phonons are equivalent to oscillations of an effective vector potential $\mathbf{A}_{\text{eff}}$ [see Eq. (7)], and therefore an effective electric field, perpendicular (parallel, respectively) to $\mathbf{q}$.

Finally, using Eqs. (10), (14), and (16) we get the dispersion relation for the LP-TO coupled mode,

$$\omega^2 - \omega_0^2 = \frac{L^2 F^2 \chi_L(\mathbf{q},\omega)}{1 - \frac{\sqrt{q^2-\omega^2/c^2}}{2\omega^2\epsilon_0}\chi_L(\mathbf{q},\omega)}, \tag{18}$$

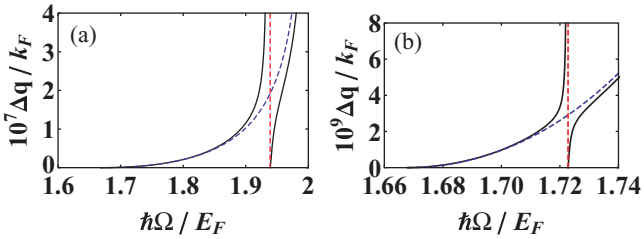

FIG. 3. (Color online) Dispersion lines of hybrid TP-LO plasmon-phonon modes (solid lines) and of the uncoupled modes (dashed lines) for two values of doping: (a) $n = 7.5 \times 10^{11}$ cm^{-2} and (b) $n = 9.5 \times 10^{11}$ cm^{-2}. The plasmonlike dispersion is very close to the light line $q = \omega/c$; therefore, the ordinate shows $\Delta q = q - \omega/c$.

and from Eqs. (11), (15), and (17) the dispersion relation for the TP-LO coupled mode,

$$\omega^2 - \omega_0^2 = \frac{L^2 F^2 \chi_T(\mathbf{q},\omega)}{1 + \frac{\mu_0}{2\sqrt{q^2-\omega^2/c^2}}\chi_T(\mathbf{q},\omega)}. \tag{19}$$

The plasmon dispersions relations (12) and (13) appear as poles in Eqs. (18) and (19) for the coupled modes, which means that the coupling is greatest at the resonance point where plasmon momentum and energy match that of the appropriate phonon mode. We denote this point (where the uncoupled plasmon and phonon dispersion cross) by (q_c,ω_0). One can quantify the strength of the coupling effect by calculating the frequency difference between the hybrid modes at the wave vector q_c in units of the uncoupled frequency value: $\Delta\omega/\omega_0$. Finally, by doping one can change plasmon dispersion which in turn changes q_c and the strength of the plasmon-phonon coupling.

The dispersion lines for the hybrid LP-TO modes are shown in Fig. 2 for two values of doping: (a) $n = 5 \times 10^{12}$ cm^{-2}, $E_F = 0.261$ eV, $k_F = 3.96 \times 10^8$ m^{-1}, and (b) $n = 5 \times 10^{13}$ cm^{-2}, $E_F = 0.825$ eV, $k_F = 1.25 \times 10^9$ m^{-1}. The strength of the coupling increases with increasing values of doping, and one has for the case (a) $\Delta\omega/\omega_0 = 7.5\%$ and (b) $\Delta\omega/\omega_0 = 15.5\%$. To describe graphene sitting on a substrate (say SiC, which is a polar material), one only needs to include the dielectric function of the substrate into our calculation. In that case plasmons can also couple to surface phonon modes of the polar substrate.[11,19,20] However, since these surface phonons have sufficiently smaller energies than optical phonons in graphene out results are qualitatively unchanged in that case. LP-TO hybrid modes could be measured by observing the change in the phonon dispersion with neutron spectroscopy or inelastic x-ray scattering. Alternatively, one could use a grating coupler or electron energy loss spectroscopy to measure the shift in the plasmon energy.

In spite of the fact that the formal derivation of hybrid TP-LO coupled modes is equivalent to the derivation of the LP-TO modes, their properties qualitatively differ. First, we note that the dispersion of TPs is extremely close to the light line, and we plot $\Delta q = q - \omega/c$ vs frequency ω following Ref. 8. For this reason, TPs are expected to have strong polariton character and they will be hard to distinguish from free photons (also, even a small plasmon linewidth will obscure the distinction). Moreover, they do not exist in graphene between two dielectrics with sufficiently different relative permittivity, where the light lines for the dielectrics are separated. Next, TPs exist only in the frequency interval $2E_F > \hbar\omega > 1.667E_F$,[8] which means that the LO phonon energy must be in the same interval for the hybridization to occur. Figure 3 shows the dispersion curves of the hybrid TP-LO modes for two values of doping: (a) $n = 7.5 \times 10^{11}$ cm^{-2}, $E_F = 0.101$ eV, $k_F = 1.53 \times 10^8$ m^{-1}, and (b) $n = 9.5 \times 10^{11}$ cm^{-2}, $E_F = 0.114$ eV, $k_F = 1.73 \times 10^8$ m^{-1}. We observe that the trend here is opposite to that of the LP-TO coupling, as the strength of the coupling decreases with increasing doping; specifically, one has for the case (a) $\Delta\omega/\omega_0 = 0.17\%$ and (b) $\Delta\omega/\omega_0 = 0.02\%$. The maximal coupling occurs when $2E_F$ is just above $\hbar\omega_0$, and it is zero when $\hbar\omega_0 = 1.667E_F$. We emphasize that the

strength of the coupling for TP-LO modes is in general much weaker than in LP-TO modes.

Before closing, we note another interesting result which is captured by our calculations. Equations (18) and (19) for shifts in the energies of TO and LO modes at $q = 0$ reduce to

$$\omega^2 - \omega_0^2 = \frac{L^2 F^2 \chi_{L,T}(0,\omega)}{1 + \frac{i}{2\omega\epsilon_0 c}\chi_{L,T}(0,\omega)}, \tag{20}$$

which is identical to the result of Ref. 4, where the coupling of optical phonons to single-particle excitations was studied, apart from the imaginary term in the denominator, which is zero in Ref. 4. This small but qualitative difference is a consequence of phonon coupling to the radiative electromagnetic modes, which increases the phonon linewidth. For example, for the doping values of $n = 5 \times 10^{12}$ cm^{-2}, 5×10^{13} cm^{-2}, and 5×10^{14} cm^{-2}, Eq. (20) yields 0.005%, 0.07%, and 0.7%, respectively, for the linewidths, while there is no linewidth from single-particle damping at these doping values. This effect is qualitatively unchanged for graphene sitting on a substrate and could be measured by Raman spectroscopy. Finally, we note an interesting solution of Eq. (19) (valid for suspended graphene): When the hybrid TP-LO mode dispersion crosses the light line it has the same energy as the uncoupled phonon mode, that is, $\omega = \omega_0$. In other words, the LO phonon at a wave vector $q = \omega_0/c$ decouples from all (single particle and collective) electron excitations, while no such effect exists for the TO phonons.

In conclusion, we have predicted hybridization of plasmons and intrinsic optical phonons in graphene using self-consistent linear response theory. We found that graphene's unique electron-phonon interaction leads to unconventional mixing of plasmon and optical phonon polarizations: Longitudinal plasmons couple exclusively to TO phonons, whereas graphene's TPs couple to LO phonons; this contrasts plasmon-phonon coupling in all previously studied systems. The strength of the hybridization increases with doping in LP-TO coupled modes, while the trend is opposite for TP-LO modes. The LP-TO coupling is much stronger than TP-LO coupling, and it could be measured by current experiments to explore the electron-phonon interaction in graphene (the frequency shifts at resonance are much larger than those recently measured by Raman spectroscopy[3]). This coupling is an even more striking example of a breakdown of Born-Oppenheimer approximation in graphene than the recently measured stiffening of the Raman G peak.[3] Moreover, plasmon-phonon interaction can serve to electronically control the frequencies of lattice vibrations in graphene, which could have interesting technological implications.

This work was supported in part by the the Croatian Ministry of Science (Grant No. 119-0000000-1015) and the MRSEC program of National Science Foundation of the USA under Award No. DMR-0819762. M.S. was also supported in part by the S3TEC, an Energy Frontier Research Center funded by the US Department of Energy, Office of Science, Office of Basic Energy Sciences, under Award No. DE-SC0001299.

*mjablan@phy.hr
†soljacic@mit.edu
‡hbuljan@phy.hr

[1] K. S. Novoselov, A. K. Geim, S. V. Morozov, D. Jiang, Y. Zhang, S. V. Dubonos, I. V. Grigorieva, and A. A. Firsov, Science **306**, 666 (2004).
[2] A. H. Castro Neto, F. Guinea, N. M. R. Peres, K. S. Novoselov, and A. K. Geim, Rev. Mod. Phys. **81**, 109 (2009).
[3] S. Pisana, M. Lazzeri, C. Casiraghi, K. S. Novoselov, A. K. Geim, A. C. Ferrari, and F. Mauri, Nat. Mater. **6**, 198 (2007).
[4] T. Ando, J. Phys. Soc. Jpn. **75**, 124701 (2006).
[5] M. Lazzeri and F. Mauri, Phys. Rev. Lett. **97**, 266407 (2006).
[6] B. Wunsch, T. Stauber, F. Sols, and F. Guinea, New J. Phys. **8**, 318 (2006).
[7] E. H. Hwang and S. Das Sarma, Phys. Rev. B **75**, 205418 (2007).
[8] S. A. Mikhailov and K. Ziegler, Phys. Rev. Lett. **99**, 016803 (2007).
[9] F. Rana, IEEE Trans. Nanotechnol. **7**, 91 (2008).
[10] C. Kramberger, R. Hambach, C. Giorgetti, M. H. Rummeli, M. Knupfer, J. Fink, B. Buchner, L. Reining, E. Einarsson, S. Maruyama, F. Sottile, K. Hannewald, V. Olevano, A. G. Marinopoulos, and T. Pichler, Phys. Rev. Lett. **100**, 196803 (2008).
[11] Y. Liu and R. F. Willis, Phys. Rev. B **81**, 081406 (2010).
[12] M. Jablan, H. Buljan, and M. Soljačić, Phys. Rev. B **80**, 245435 (2009).
[13] B. B. Varga, Phys. Rev. **137**, A1896 (1965).
[14] A. Mooradian and G. B. Wright, Phys. Rev. Lett. **16**, 999 (1966).
[15] R. Matz and H. Lüth, Phys. Rev. Lett. **46**, 500 (1981).
[16] Wu Xiaoguang, F. M. Peeters, and J. T. Devreese, Phys. Rev. B **32**, 6982 (1985).
[17] L. Wendler and R. Pechstedt, Phys. Rev. B **35**, 5887 (1987).
[18] R. Jalabert and S. Das Sarma, Phys. Rev. B **40**, 9723 (1989).
[19] E. H. Hwang, R. Sensarma, and S. Das Sarma, Phys. Rev. B **82**, 195406 (2010).
[20] R. J. Koch, Th. Seyller, and J. A. Schaefer, Phys. Rev. B **82**, 201413(R) (2010).
[21] This result is in contrast to that of W-K. Tse, Ben Yu-Kuang Hu, and S. Das Sarma, Phys. Rev. Lett. **101**, 066401 (2008), which predicts no coupling at all. The statement given in that paper about vanishing of hybrid bubbles is valid only for LO but not for TO phonons.
[22] P. R. Wallace, Phys. Rev. **71**, 622 (1947).
[23] G. W. Semenoff, Phys. Rev. Lett. **53**, 2449 (1984).
[24] H. Suzuura and T. Ando, Phys. Rev. B **65**, 235412 (2002).
[25] K. Ishikawa and T. Ando, J. Phys. Soc. Jpn. **75**, 084713 (2006).
[26] D. Pines and P. Nozieres, *The Theory of Quantum Liquids* (Benjamin, New York, 1966).
[27] A. Principi, M. Polini, and G. Vignale, Phys. Rev. B **80**, 075418 (2009).
[28] L. A. Falkovsky and A. A. Varlamov, Eur. Phys. J. B **56**, 281 (2007).